

# Calculation of Electric Potentials Transferred by Grounding Systems

Rooney R. A. Coelho<sup>\*</sup> Mauricio B. C. Salles<sup>†\*</sup>  
Luciano Martins Neto<sup>‡</sup> José Roberto Cardoso<sup>\*</sup>

<sup>\*</sup> *Laboratory of Applied Electromagnetics (LMAG)  
Polytechnic School of the University of São Paulo, São Paulo, Brazil*

<sup>†</sup> *Laboratory of Advanced Electric Grids (LGrid)  
Polytechnic School of the University of São Paulo, São Paulo, Brazil*

<sup>‡</sup> *Federal University of Uberlândia, Minas Gerais, Brazil*

e-mails: rooneycoelho@usp.br, mausalles@usp.br, lmn@ufu.br,  
jose.cardoso@usp.br

**Abstract:** Buried metal elements such as fences, pipelines, building rebar, and railway tracks are subject to electric potential rise due to current flowing through the ground. In fact, there may be a potential transfer of substations to remote regions in which such safety risks are not generally expected. This work presents a calculation procedure for this potential rise in uniform soils. The presented procedure is applied to cases extracted from the literature as a form of validation.

**Keywords:** Grounding; Uniform soil; Floating potential; Substations; Numerical methods.

## 1. INTRODUCTION

This article addresses a very important engineering problem in the area of electrical grounding, which is the study of potentials transferred to other conductors located near a grounding system. For Colominas et al. (2005), such potentials can reach remote points through communication circuits, neutral wires, pipes, rails or metallic fences. This effect can produce serious safety issues that must somehow be studied.

Buried metal bodies are under the same electric potential, regardless of whether there is a current injection in them. If there is a metal body in the vicinity of a grounding system, where a short circuit current flows to the ground, the potential in this metallic body is a function of the current intensity, geometry and distance to the grounding system. It can be stated that the potential in the body has been "transferred" from the grounding system through the soil. Such a problem can also be understood as a conductive coupling between the grounding system and the metallic body.

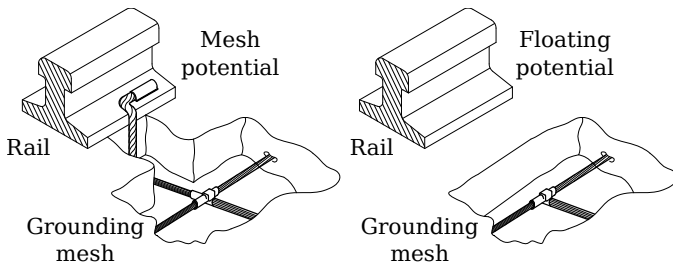


Figure 1. Electric Potential on a metallic rail when connected to the mesh (left) and not connected (right).

An interesting situation to illustrate the problem of transferred potentials is the case of metallic rails in the vicinity of a substation. As shown in Figure 1, even when this rail is not directly connected to the grounding mesh, there will be a potential rise on this rail due to the passage of the electric current on the soil. The rail has a floating potential, being unknown and it needs to be somehow calculated. The mesh or rails connected to this mesh can be referred to as active electrodes, where there is a current injection, and a disconnected rail as a passive electrode, where there is no current injection.

This article presents a calculation procedure for the current distribution and potential rise in active and passive electrodes, as well as its application in the determination of transferred potentials, in particular to substation external areas.

## 2. EQUATIONING

For the study of the potential rise in passive electrodes, it is necessary to initially develop a model for the grounding system, especially for the calculation of electric potential and current distribution.

### 2.1 Linear electrode electric potential

The electric potential with the zero reference in infinity generated by a point current source  $I$ , immersed in a uniform soil of resistivity  $\rho$  is given by

$$V(\mathbf{r}) = \frac{\rho I}{4\pi} \left( \frac{1}{\mathcal{R}} + \frac{1}{\mathcal{R}'} \right), \quad (1)$$

with  $r_{xy} = \sqrt{(x - x')^2 + (y - y')^2}$ , where  $\mathbf{r}$  is the vector position for the calculation point. Distances from the

current source and image source to the calculation point are respectively

$$\mathcal{R} = \sqrt{r_{xy}^2 + (z - z')^2} \quad \text{e} \quad \mathcal{R}' = \sqrt{r_{xy}^2 + (z + z')^2}.$$

As demonstrated in Coelho (2019), the image method used in electrical grounding problems differs from those of electrostatics. In electrostatic problems, it is sought to obtain the effect of stationary charges in the vicinity of conductive planes, whose field lines are normal to the interface. For the problem in question, there is a point current source in a conductive medium and it is necessary to obtain the effect of the soil-air interface. Therefore, it is aimed to obtain tangential lines to model this interface, for such, there is no signal inversion for the image source.

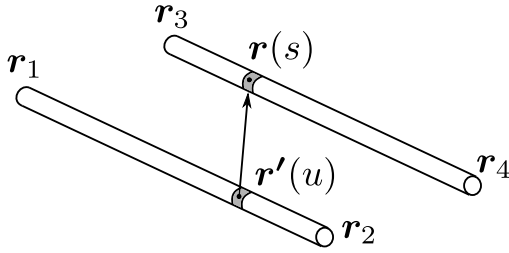


Figure 2. Calculation of the potential generated by a conductor, located between  $\mathbf{r}_1$  and  $\mathbf{r}_2$ , on a nearby conductor (surface), located between  $\mathbf{r}_3$  and  $\mathbf{r}_4$ .

Now taking a segment of length  $L$  and with uniform current density per unit length rather than a point source, the potential generated by the point source can be integrated along a trajectory between coordinates  $\langle x_1, y_1, z_1 \rangle$  and  $\langle x_2, y_2, z_2 \rangle$ , which respectively represent its beginning and end points. Using vector notation, this same element can be described as bounded by  $\mathbf{r}_1$  and  $\mathbf{r}_2$ . Any point of the parameterized segment in  $u$  is then obtained by  $u\mathbf{r}_1 + (1 - u)\mathbf{r}_2$  for  $u \in [0, 1]$  (cf. Figure 2). After calculating such line integral in the parameter  $u$ , the resulting potential is then obtained by (2) (Coelho, 2019).

$$V(\mathbf{r}) = \frac{\rho I}{4\pi L} \left( \ln \left| \frac{2a + b + 2\sqrt{a(a + b + c)}}{b + 2\sqrt{ac}} \right| + \ln \left| \frac{2a' + b' + 2\sqrt{a'(a' + b' + c')}}{b' + 2\sqrt{a'c'}} \right| \right), \quad (2)$$

being the auxiliary functions for the real source

$$a = a' = (x_2 - x_1)^2 + (y_2 - y_1)^2 + (z_2 - z_1)^2 = L^2$$

$$b(x, y, z) = 2(z_1 - z)(z_2 - z_1) + 2(y_1 - y)(y_2 - y_1) + 2(x_1 - x)(x_2 - x_1)$$

$$c(x, y, z) = (x - x_1)^2 + (y - y_1)^2 + (z - z_1)^2,$$

and for image source

$$b'(x, y, z) = 2(-z_1 - z)(z_1 - z_2) + 2(y_1 - y)(y_2 - y_1) + 2(x_1 - x)(x_2 - x_1)$$

$$c'(x, y, z) = (x - x_1)^2 + (y - y_1)^2 + (z + z_1)^2.$$

Observe that once (2) is parameterized based on segment coordinates, this equation can be used to calculate the electric potential generated by a cable, rod, or even an inclined electrode. Hitherto, there is a parameter in (2) that must be imposed, which is the electric current injected into the electrode. When there is a system with multiple electrodes

the current distribution between them is non-uniform and is calculated in such a way that the association becomes equipotentialized.

## 2.2 Multiple electrode systems

Equation (2) allows the calculus of the electric potential once the segment current is known. If there is more than one electrode in the system, due to the superposition principle, the calculation of the electric potential for such association is made by adding the effect of each electrode isolatedly. However, when there is an association of electrodes, the current distribution depends on the geometry of the problem and must be determined in advance for the correct calculation of the whole system electric potential.

Once the electrodes are formed by a conductive surface, it is known that such surface is equipotential, being interconnected conductors also under the same potential. By applying the superposition theorem, it is possible to determine every electrode current that satisfies the equipotentiality condition. The potential rise generated by a segment  $i$  on the surface of a segment  $j$ , for a still to be determined current in  $i$ , can be calculated by integration, as illustrated by Figure 2. Since the segment  $j$  is delimited between  $\mathbf{r}_3$  and  $\mathbf{r}_4$ , any point in this element can be parameterized as  $s\mathbf{r}_3 + (1 - s)\mathbf{r}_4$  for  $s \in [0, 1]$ . The ratio between the potential rise in the segment  $j$  by the current that generated this elevation (coming from the segment  $i$ ) is known as the mutual resistance between segments and is given by the following numerical integration

$$R_{ij} = \frac{\rho}{4\pi L} \int_0^1 \left( \ln \left| \frac{2a + b(s) + 2\sqrt{a(a + b(s) + c(s))}}{b(s) + 2\sqrt{ac(s)}} \right| + \ln \left| \frac{2a' + b'(s) + 2\sqrt{a'(a' + b'(s) + c'(s))}}{b'(s) + 2\sqrt{a'c'(s)}} \right| \right) ds. \quad (3)$$

Cases in which  $i = j$  represents the calculation of a segment own resistance and there is a singularity in (2). This is because the thickness of the element was not considered in the electric potential formulation. Once the calculation point should be taken on the surface of the element instead of in its central axis, the correction of ((4) is used for such coordinates.

$$\begin{aligned} x_3 &= x_1 + r_c \frac{y_2 - y_1}{L} & x_4 &= x_2 + r_c \frac{y_2 - y_1}{L} \\ y_3 &= y_1 + r_c \frac{z_2 - z_1}{L} & y_4 &= y_2 + r_c \frac{z_2 - z_1}{L} \\ z_3 &= z_1 + r_c \frac{x_2 - x_1}{L} & z_4 &= z_2 + r_c \frac{x_2 - x_1}{L} \end{aligned} \quad (4)$$

Once this is done, the offset of the calculation point is equal to the radius of the element  $r_c$ , regardless of the segment space orientation.

The potential rise  $V_0$  calculated in a segment  $i$  is the superposition of effects of all  $N$  segments in this element.

$$\sum_{j=1}^N R_{ij} I_j = V_0 \quad \text{ou} \quad \sum_{j=1}^N R_{ij} I_j - V_0 = 0 \quad (5)$$

By the current continuity equation, it is known that the sum of currents flowing through each electrode is equal to the total current  $i_{cc}$  injected into the system.

$$\sum_{i=1}^N I_i = I_{cc} \quad (6)$$

As done in Pereira F<sup>o</sup> and Cardoso (2001), applying the form used in (5) to all system electrodes and combining (6), the linear system equation (7) is obtained, whose solution provides the electrodes current distribution and also the electric potential in such electrodes for the total current injected into the system.

$$\begin{bmatrix} R_{11} & R_{12} & R_{13} & \cdots & -1 \\ R_{21} & R_{22} & R_{23} & \cdots & -1 \\ R_{31} & R_{32} & R_{33} & \cdots & -1 \\ \vdots & \vdots & \vdots & \ddots & \vdots \\ 1 & 1 & 1 & \cdots & 0 \end{bmatrix} \cdot \begin{bmatrix} I_1 \\ I_2 \\ I_3 \\ \vdots \\ V_0 \end{bmatrix} = \begin{bmatrix} 0 \\ 0 \\ 0 \\ \vdots \\ I_{cc} \end{bmatrix} \quad (7)$$

Once each electrode current is known, the electric potential at any point of space is calculated by the superposition of (2) for each system electrode. The grounding resistance of the system is obtained by the ratio between electrodes potential  $V_0$  and the total current  $I_{cc}$  injected into the system.

### 2.3 Systems with passive electrodes

Passive electrodes are buried metal bodies that are not directly connected with the grounding system; however, there is a potential rise in these elements induced by the passage of current through soil. Examples of passive electrodes are metal fences (not connected to the grounding system), metal pipes (e.g., water, gas, oil), building rebars, train rails as well as other grounding systems.

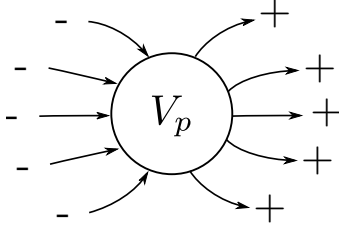


Figure 3. The sum of currents in a passive electrode is null and there is a floating potential  $V_p$  in such electrode.

Once passive electrodes are metallic, they are under the same electric potential, which is a function of distance, the injected current magnitude, and geometry of the system that generated such potential. It is common to refer to the potential of passive electrodes as a floating potential.

The passive electrode model is based on the continuity equation (8), as described in Cardoso (2010). Passive electrodes do not represent sources or sinks for the problem, i.e., they are inert elements, for this reason in (8) the sum of currents is adopted as null.

$$\oint \mathbf{J} \cdot d\mathbf{S} = \sum_{k=1}^{N_p} I_k = 0 \quad (8)$$

The calculation of the floating potential at passive electrodes includes the superposition of the effects of every segment, i.e. active and passive.

$$\sum_{j=1}^{N_a+N_p} R_{kj} I_j = V_p \quad \text{ou} \quad \sum_{j=1}^{N_a+N_p} R_{kj} I_j - V_p = 0 \quad (9)$$

There are  $N_a$  active and  $N_p$  passive electrodes, where  $V_p$  is the floating potential.

Figure 3 illustrates the inert element model with floating potential behaviour. For the model of passive electrodes, different from the one performed for active electrodes, the current distribution through electrodes can also assume negative values, as long as the total sum of the currents is null. For a better representation of such current distribution in passive electrodes, it is necessary to segment such elements, since the equation presented in this paper assumes a uniform current on each segment, which is not a suitable model for long electrodes. Each segmented element is equipotential despite its diameter because the potential gradient occurs over elements' length.

For the introduction of passive electrodes in (7), as presented in Pereira F<sup>o</sup> (1999), the following steps are carried out:

- (1) It is calculated the mutual resistance between active, passive, and between both kinds of electrodes. The penultimate column for each row is equal to -1 if the line index is referring to an active electrode or 0 when such electrode is passive. The last column for each of these rows is equal to 0 if the line index is referring to an active electrode or -1 for the passive case.
- (2) In the resistances matrix, penultimate row is assigned 1 case the column index is referring to an active electrode or 0 for the passive case. The last column of this row is always null.
- (3) In the resistances matrix last line, one does the opposite, one assigns 1 when the column index refers to a passive electrode or 0 for an active. The last column of this row is always null.

Equation (10) presents the described linear system construction rule. It is assumed  $V_a$  as the potential in active electrodes and  $V_p$  as the potential in passive e electrodes. In this equation, the term with index  $k$  refers to a passive electrode, with the other terms referring to active electrodes. If the passive electrode is segmented, a different current is calculated for each segment, increasing the system order. It was decided to assemble the matrix starting with terms referenced to active electrodes, which were related to currents indexed from 1 to  $N_a$ . Passive electrodes are inserted in sequence, referring to currents indexed from  $N_a + 1$  to  $N_a + N_p$ , the system has an order of  $N_a + N_p + 2$ . The  $I_{cc}$  variable of (10) is the system's total injected current, such as a short circuit current injected at the active electrodes. The system lines can be exchanged, however, it was decided to proceed the aforementioned way, systematizing the interpretation of active and passive electrodes.

$$\begin{bmatrix} R_{11} & R_{12} & R_{13} & \cdots & R_{1k} & \cdots & -1 & 0 \\ R_{21} & R_{22} & R_{23} & \cdots & R_{2k} & \cdots & -1 & 0 \\ R_{31} & R_{32} & R_{33} & \cdots & R_{3k} & \cdots & -1 & 0 \\ \vdots & \vdots & \vdots & \ddots & \vdots & \vdots & \vdots & \vdots \\ R_{k1} & R_{k2} & R_{k3} & \cdots & R_{kk} & \cdots & 0 & -1 \\ \vdots & \vdots & \vdots & \ddots & \vdots & \vdots & \vdots & \vdots \\ 1 & 1 & 1 & \cdots & 0 & \cdots & 0 & 0 \\ 0 & 0 & 0 & \cdots & 1 & \cdots & 0 & 0 \end{bmatrix} \cdot \begin{bmatrix} I_1 \\ I_2 \\ I_3 \\ \vdots \\ I_k \\ \vdots \\ V_a \\ V_p \end{bmatrix} = \begin{bmatrix} 0 \\ 0 \\ 0 \\ \vdots \\ 0 \\ \vdots \\ I_{cc} \\ 0 \end{bmatrix} \quad (10)$$

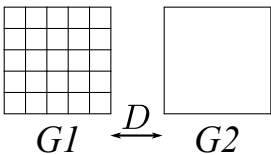
Another reason for explaining the previously described sequence is to aid the reading of coordinates of the grounding system through a Computer-Assisted Drawing (CAD) file. Every segment coordinate, both active and passive is obtained by interpreting such file. Active and passive electrodes differ through the drawing layer each line segment is labelled. The interpretation of coordinates through a CAD file enables the simulation of generic systems with complex geometries.

### 3. RESULTS

#### 3.1 Case study A

The first case study was based on data extracted from Parise et al. (2015), this article takes a hypothetical grounding system, formed by a 5 x 5 squares of 2 m side length reticulate, excited by a short-circuit current. Another grounding system is also taken in the vicinity of the aforementioned, composed of a single square of 10 m length side. The active system is identified as  $G_1$  and the passive as  $G_2$ , only the active system is directly crossed by the fault current. The resistance of both grounding systems  $R_{G1}$  and  $R_{G2}$  are then calculated, such as the mutual resistance  $R_m$  between both systems. The mutual resistance for a segment association can be calculated as the ratio between the potential rise in passive conductors and the current that generated such potential. The current injection point for a low-frequency simulation does not matter because propagation effects are neglected. However, the best injection point is the center of the mesh. The mesh segmentation is performed such that elements do not overlap, i.e. conductors' joints.

Table 1. Mutual resistance between two grounding systems.



$D$ (m)	$R_m$ ( $\Omega$ )	Parise et al. (2015)	$\Delta R_m$ (%)
5	1.141	1.139	0.165
10	0.827	0.826	0.110
15	0.652	0.652	0.052
20	0.540	0.539	0.116
25	0.460	0.460	0.109
30	0.402	0.400	0.445

The adopted soil is uniform with electric resistivity of 100  $\Omega.m$ , the conductors which form meshes were adopted as 7.67 mm diameter. The passive electrode was segmented into four elements, one for each side of a square mesh, each of them with uniform current. Table 1 presents the mutual resistance calculated for several distances  $D$  between both systems, as illustrated by the presented diagram. Furthermore, such table also presents the percentage deviation of  $\Delta R_m$  between the values calculated in this paper and the values obtained in Parise et al. (2015).

The calculated grounding resistance values were 4.367  $\Omega$  for  $R_{G1}$  and 5.546  $\Omega$  for  $R_{G2}$ . The values obtained by Parise et al. (2015) were 4.310  $\Omega$  to  $R_{G1}$  and 5.440  $\Omega$

for  $R_{G2}$ , note that such values agree with the proposed solution. These values have no significant dependence on the distance between grounding systems since they are not connected.

To exemplify the applicability of such problem, take as an example the case in which the distance  $D$  between systems is 30 m, as  $R_m = 0.402 \Omega$  for this case, being  $G_1$  excited by a hypothetical fault current of  $I_1 = 1$  kA, a  $R_m I_1 = 401.787$  V voltage will be induced at  $G_2$ , even if both systems are not interconnected.

Table 1 example can serve as a calculating basis for the potential rise in a building grounding system at the vicinity of a substation. Such systems are made through a grounding ring around the construction, a similar configuration to that of the current case study. This potential rise can lead to risks for people and even influence the operation of sensitive electronic equipment.

#### 3.2 Case study B

A railway spur (cf. Figure 4) is commonly installed in the vicinity of large substations and generating plants to facilitate the transportation and installation of large transformers and general equipment. This example was extracted from Colominas et al. (2005), which aims on the calculation of induced electric potential in a railway system near a grounding system. The potential rise on the rail was considered due to conductive coupling between the systems or by interconnection to the grounding system.

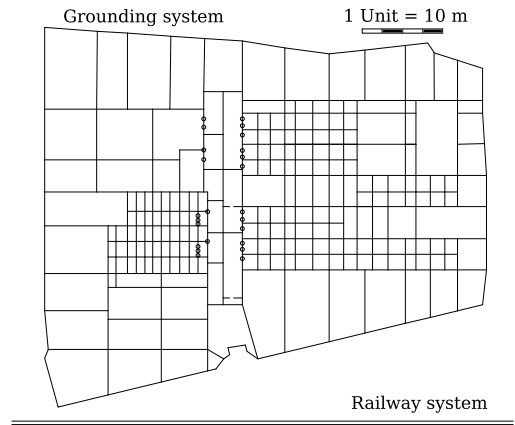


Figure 4. Problem analyzed in Case Study B.

According to Silva et al. (1999), when designing a rail transport system, whatever railway or subway line, the system user must be fully protected from electric shocks. Because the railroad rail is metallic, it can transfer dangerous potentials to remote locations due to fault conditions, implying an intolerable risk to people's safety.

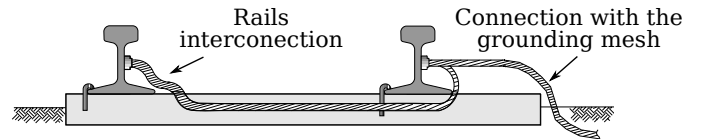


Figure 5. The rails are connected to each other and electrically connected to the grounding system.

A comparative study is carried out with the grounding system of Figure 4, composed of cables and 4 m long

rods (circles in Figure), buried at 0.75 m depth under a uniform soil with  $60 \Omega.m$  of resistivity. Since (10) is a linear system, any value of resistivity is allowed with no restriction for high resistivity soils. There are two 260 m long rails, separated by a distance of 1.668 m. Each rail is modelled as a half-buried cylinder of 94 mm diameter.

This study considers the case in which the railway system is directly connected to the grounding mesh, according to Figure 5 scheme, adapted from Switzer (1999), both rails also interconnected. A case considering only a connection between rails and not to the grounding mesh is also considered, in such case, the rails represent a floating potential.

For better accuracy in modelling rails as well as in passive elements, each one was segmented into 50 elements, the sum of the total currents of the two rails was adopted as null, which represents that both rails are under the same floating potential. The potential of each rail can also be calculated separately by adapting (10) for multiple floating potentials, each of them, whose sum of the currents being null. Figure 6 shows the current calculated in each segment of both rails, the initial indices represent the segments closest to the substation mesh, those currents are the result of (10) for currents associated with a floating potential.

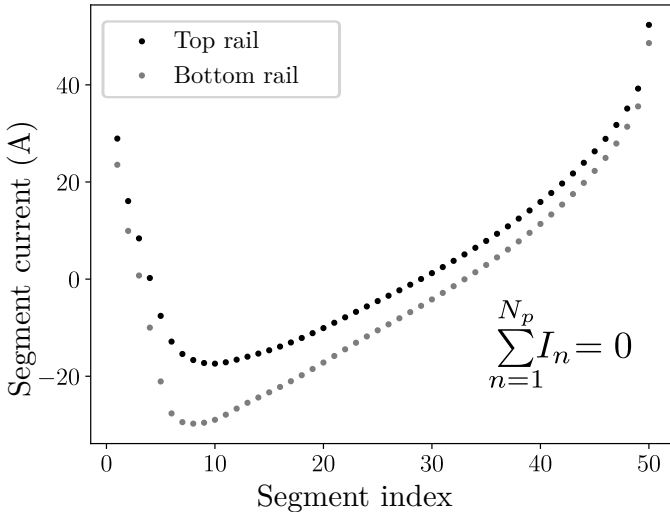


Figure 6. Current distribution at the railway system considering a floating potential. Both rails were considered under the same potential.

It is initially considered that the rail and grounding mesh are not connected. The calculated grounding resistance of the mesh is  $0.1477 \Omega$ . In comparison, the value of  $0.1482 \Omega$  was obtained in the original article. The calculated mutual resistance is  $0.0780 \Omega$ . The potential rise ratio between mesh and rail is 0.528, being 0.516 the original article value.

For a short circuit current of 67.47 kA in the grounding system, as reported in the article, there will be a potential rise of 9.80 kV in the mesh and a transferred potential of 5.17 kV throughout the length of the rails. Considering the potential rise on each rail individually (rather than both rails under the same potential) a voltage of 90.61 V is reached between both tracks. The potential induced in the tracks takes a hazardous situation to areas away from

the substation, where appropriate protective and signaling equipment like those existing in a substation area is often lacking.

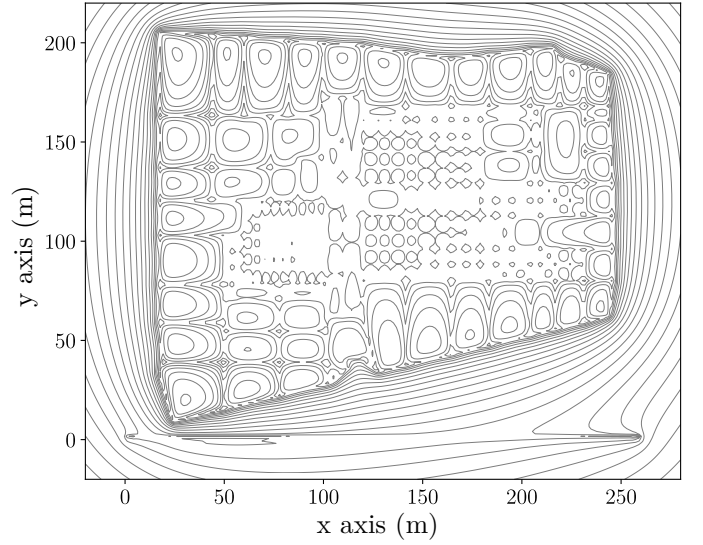


Figure 7. Equipotential lines on the soil surface for grounding mesh and non-interconnected rails.

Figure 7 illustrates the behaviour of the electric potential on the soil surface for Figure 4 scheme for the case where the systems are not interconnected. The grounding mesh is segmented on conductors' joints and rails are uniformly segmented along their length with 50 segments each. It is possible to observe the deformation on the equipotential lines due to rail tracks. The more concentrated the equipotential lines are, the greater the existing step voltage. On the other hand, the touch potential is characterized by the difference between the potential of the mesh, or a floating potential, and a point on the soil surface that represents the reach of a person's arm.

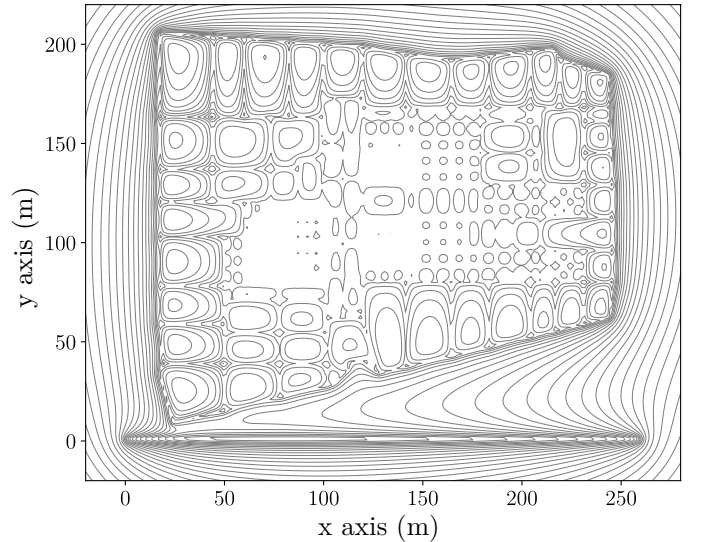


Figure 8. Equipotential lines at the soil surface for grounding mesh and interconnected rails.

The calculated grounding resistance when rails are connected to the mesh is  $0.1365 \Omega$ , exactly the same value that was obtained by Colominas et al. (2005). Note that the

grounding resistance for this configuration is lower because the rails are active electrodes, thus increasing the effective area of the grounding system. The rails potential for this case is the same as the grounding mesh since both are interconnected.

For the same current of 67.47 kA at the grounding system, when connected to the rails it has a potential rise of 9.21 kV, which is lower than the potential when the rail is not connected to the mesh. However, all this potential is fully transferred to the rail.

When only a lower grounding resistance is sought, designers may tend to adopt this solution, however, the risk of such a practice should also be taken into account. Whenever a grounding system is interconnected with a nearby electrode such as roads, construction rebar, it is necessary to weigh the risks of transporting such potentials to remote areas and not only aim to reduce the grounding resistance.

Figure 8 illustrates the behavior of electric potential on the soil surface for Figure 4 scheme, in which case rail tracks are directly connected to the mesh. The grounding mesh is segmented on conductors' joints and rails are uniformly segmented along their length with 50 segments each. For this configuration, the rails are an active part of the grounding system. What can be observed by the change in the pattern of equipotential lines, being the mesh and rails subject to the same electric potential. When compared with Figure 7, where there is no interconnection, it is possible to observe that there is an increase in the concentration of equipotential lines in the vicinity of the tracks, being an even more dangerous situation than the previously analyzed one.

#### 4. CONCLUSION

In this article, a physical model for low frequency electric current dissipation is presented for uniform soils. Such a model can be applied for short-circuit studies and switching manoeuvres in power systems. However, for atmospheric discharge studies, it is necessary to readapt the presented model through a current dissipation such as Alípio et al. (2011).

This work presents a method for calculating induced potentials due to resistive couplings for generic grounding configurations, a procedure that can be applied to various problems such as calculating induced potentials in metallic fences, building grounding rings, nearby substations, train tracks, among other configurations.

The method approached in this article was applied in practical cases extracted from the literature, suggested results were similar to original papers, even using different approaches. It is worth mentioning the simplicity and generalization capabilities of the method presented in this article, which allow the study of complex geometries and practical problems, as well as a possible adaptation to heterogeneous soils as well as high frequency currents.

#### REFERENCES

Alípio, R.S., Schroeder, M.A.O., Afonso, M.M., and Oliveira, T.A.S. (2011). Modelagem de aterramentos

- elétricos para fenômenos de alta frequência e comparação com resultados experimentais. *Revista Controle & Automação (SBA)*, 22(1), 89–102.
- Cardoso, J.R. (2010). *Engenharia eletromagnética*. Elsevier, Rio de Janeiro, 1 edition.
- Coelho, R.R.A. (2019). *Uma contribuição à análise de sistemas de aterramento em meios horizontalmente estratificados*. Ph.D. thesis, Universidade Federal de Uberlândia. doi:10.14393/ufu.te.2019.2045. In portuguese.
- Colominas, I., Navarrina, F., and Casteleiro, M. (2005). Analysis of transferred earth potentials in grounding systems: a bem numerical approach. *IEEE Transactions on Power Delivery*, 20(1), 339–345. doi:10.1109/TPWRD.2004.835035.
- Parise, G., Parise, L., and Martirano, L. (2015). The interference of grounding systems: The floating behavior. *IEEE Transactions on Industry Applications*, 51(6), 5038–5043. doi:10.1109/TIA.2015.2443093.
- Pereira F<sup>o</sup>, M.L e Cardoso, J.R. (2001). Avaliação de desempenho de malhas de terra usando imagens complexas: uma nova abordagem. *Controle & Automação (SBA)*, 12, 215–223.
- Pereira F<sup>o</sup>, M.L. (1999). *Aplicação do método das imagens complexas ao cálculo de malhas de aterramento em solos com estratificação horizontal*. Master's thesis, Escola Politécnica, Universidade de São Paulo- USP. doi:10.11606/D.3.1999.tde-30112004-171403.
- Silva, J.A.P., Cardoso, J.R., Guirelli, C.R., and Rossi, L.N. (1999). Uma formulação Íntegro-diferencial de 4a. ordem aplicada à simulação de sistemas de aterramento metro-ferroviários. *Controle & Automação (SBA)*, 10(3), 176–182.
- Switzer, W.K. (1999). Practical guide to electrical grounding. *An ERICO Publication First Printing*.